**RESEARCH ARTICLE**

# Endo-lysosomal TRP mucolipin-1 channels trigger global ER Ca²⁺ release and Ca²⁺ influx

Bethan S. Kilpatrick[1],*, Elizabeth Yates[1],*, Christian Grimm[2], Anthony H. Schapira[3] and Sandip Patel[1],‡

## ABSTRACT

Transient receptor potential (TRP) mucolipins (TRPMLs), encoded by the MCOLN genes, are patho-physiologically relevant endo-lysosomal ion channels crucial for membrane trafficking. Several lines of evidence suggest that TRPMLs mediate localised Ca²⁺ release but their role in Ca²⁺ signalling is not clear. Here, we show that activation of endogenous and recombinant TRPMLs with synthetic agonists evoked global Ca²⁺ signals in human cells. These signals were blocked by a dominant-negative TRPML1 construct and a TRPML antagonist. We further show that, despite a predominant lysosomal localisation, TRPML1 supports both Ca²⁺ release and Ca²⁺ entry. Ca²⁺ release required lysosomal and ER Ca²⁺ stores suggesting that TRPMLs, like other endo-lysosomal Ca²⁺ channels, are capable of 'chatter' with ER Ca²⁺ channels. Our data identify new modalities for TRPML1 action.

KEY WORDS: Ca²⁺, Lysosomes, TRP channels, Endoplasmic reticulum

## INTRODUCTION

The remarkable versatility of Ca²⁺ as an intracellular messenger is underpinned by the spatiotemporal organisation of Ca²⁺ signals (Berridge et al., 2003). Targeted delivery of Ca²⁺ to a particular subcellular locale is one way in which Ca²⁺ can selectively influence a particular cell outcome (e.g. secretion). Equally, global Ca²⁺ signals, which are often oscillatory, can also be selective through information encoded in oscillation frequency. Interplay between Ca²⁺ release from intracellular Ca²⁺ stores and Ca²⁺ influx from the extracellular space ensures tight control of Ca²⁺ levels and their downstream targets (Clapham, 2007). Although we have gained much mechanistic insight into the mobilisation of ER Ca²⁺ stores and the subsequent entry of Ca²⁺ across the plasma membrane that ensues (Prakriya and Lewis, 2015), we know relatively little about Ca²⁺ handling by acidic Ca²⁺ stores such as lysosomes (Patel and Muallem, 2011).

Lysosomes are best known for their degradative role but they maintain an intraluminal Ca²⁺ concentration (∼500 µM) similar to

[1]Department of Cell and Developmental Biology, University College London, Gower Street, London WC1E 6BT, UK. [2]Center for Integrated Protein Science CIPSM and Department of Pharmacy – Center for Drug Research, Ludwig-Maximilians-Universität München, München 81377, Germany. [3]Department of Clinical Neurosciences, Institute of Neurology, University College London, London NW3 2PF, UK.
*These authors contributed equally to this work

‡Author for correspondence (patel.s@ucl.ac.uk)

S.P., 0000-0001-7247-2013

the ER (Christensen et al., 2002; Lloyd-Evans et al., 2008). They are likely filled by Ca²⁺-H⁺ exchange (Melchionda et al., 2016) and express members of the transient receptor potential mucolipin (TRPML) and two-pore channel (TPC) families to effect Ca²⁺ release (Grimm et al., 2012; Kiselyov et al., 2012; Patel, 2015; Waller-Evans and Lloyd-Evans, 2015). Three TRPML isoforms are present in humans (García-Añoveros and Wiwatpanit, 2014). TRPML1 (encoded by MCOLN1) is ubiquitously expressed and targets to lysosomes through di-leucine motifs (Vergarajauregui and Puertollano, 2006). It is activated by the endo-lysosomal phosphoinositide phosphatidylinositol 3,5-bisphosphate [PI(3,5)P₂] (Dong et al., 2010) and is a non-selective cation channel permeable to a number of ions including Ca²⁺ and Fe²⁺ (Dong et al., 2008). Importantly, mutation of TRPML1 results in the lysosomal storage disorder mucolipidosis type IV (Bargal et al., 2000). This neurodegenerative disorder is characterised by build-up of various lipid species in lysosomes, suggesting a role for TRPML1 in lipid trafficking. It has long been recognised that localised Ca²⁺ release from the endo-lysosomal system can influence vesicular fusion and fission events (Pryor et al., 2000). Specifically, Ca²⁺ release through TRPMLs likely underlies functional roles in vesicular trafficking as well as lysosomal exocytosis (Samie et al., 2013), autophagy (Medina et al., 2015) and regulated secretion (Park et al., 2016). Notably, recently described TRPML agonists have proven beneficial in correcting trafficking defects not only in mucolipidosis type IV (Chen et al., 2014) but also in Niemann–Pick type C disease (Shen et al., 2012) and HIV-associated dementia (Bae et al., 2014). Defective TRPML activity has also been implicated in Alzheimer's disease (Lee et al., 2015). Despite their demonstrable (patho)physiological relevance, TRPML-mediated Ca²⁺ signals are difficult to resolve due to their localised nature. To overcome this, a number of recent studies have used genetically encoded Ca²⁺ indicators such as GCaMP-3 or GECO fused directly to TRPML1 to record Ca²⁺ signals in response to agonist activation (Bae et al., 2014; Cao et al., 2015; Medina et al., 2015; Shen et al., 2012). These signals are suggested to reflect local peri-lysosomal Ca²⁺ release. But it is not clear how the relatively high-affinity Ca²⁺ indicators used distinguish between local and global Ca²⁺ signals.

In addition to supporting local Ca²⁺ fluxes required for endocytic 'well-being' (Hockey et al., 2015), lysosomes can also initiate global Ca²⁺ signals during signalling. This process has been established in the context of the actions of the messenger nicotinic acid adenine dinucleotide phosphate (NAADP) (Galione, 2015). According to the trigger hypothesis, increases in NAADP levels activate endo-lysosomal Ca²⁺ channels, generating local Ca²⁺ signals that sensitise neighbouring Ca²⁺ release channels on the ER. Activation of the latter (on the more substantial store) results in global Ca²⁺ release. Indeed, in fibroblasts, direct mobilisation of lysosomal Ca²⁺ stores through osmotic permeabilisation is sufficient to trigger ER-dependent complex Ca²⁺ signals

(Kilpatrick et al., 2013). Physiologically, it is the TPCs that have emerged as the target channels for NAADP (Brailoiu et al., 2009; Calcraft et al., 2009; Patel, 2015) although a role for TRPMLs has also been advanced (Zhang et al., 2011, but see Yamaguchi et al., 2011). Coupling between TPCs and ER $Ca^{2+}$ channels likely occurs at membrane contact sites between lysosomes and the ER (Kilpatrick et al., 2013; Patel and Brailoiu, 2012; Penny et al., 2014). Although TRPMLs can evoke global $Ca^{2+}$ entry, at least when mutated as exemplified by the Va mutation in TRPML3 (encoded by *MCOLN3*) (Grimm et al., 2007; Kim et al., 2007), whether they support lysosome–ER cross talk is not known.

Here, we take advantage of TRPML agonists ML-SA1 (Shen et al., 2012) and MK6-83 (Chen et al., 2014) to probe the $Ca^{2+}$ permeability of TRPMLs in an intact cell setting. We show that activation of TRPML1 unexpectedly evokes global $Ca^{2+}$ signals. Mechanistically, we dissect these signals into release and influx components implicating both ER and extracellular $Ca^{2+}$, in addition to lysosomal $Ca^{2+}$, for their genesis. Our data suggest that the action of TRPML1 is not limited to local lysosomal $Ca^{2+}$ signalling.

## RESULTS

### TRPML agonists evoke global $Ca^{2+}$ signals

Fusion proteins comprising TRPML1 and either GCaMP-3 (Shen et al., 2012) or GECO (Cao et al., 2015) have been used to resolve presumed local $Ca^{2+}$ fluxes from lysosomes upon TRPML1 activation. But as shown in Fig. 1A and Movie 1, $Ca^{2+}$ responses to ML-SA1 (20 µM) were readily resolvable in a proportion of Hela cells loaded with the fluorescent $Ca^{2+}$ indicator Fura-2. This organic dye distributes throughout the cytosol and thus records bulk changes in cytosolic $Ca^{2+}$. ML-SA1 responses were concentration dependent (Fig. 1A). Similar results were obtained using primary cultured human fibroblasts. As in HeLa cells, ML-SA1 evoked strong $Ca^{2+}$ responses in Fura-2-loaded cells in a concentration-dependent manner (Fig. 1B; Movie 2). The amplitude of the $Ca^{2+}$ signals and the proportion of responsive cells are quantified in Fig. 1C,D. Fibroblasts were more responsive than HeLa cells, although we noted considerable variability between experiments, particularly for fibroblasts (Fig. 1D). To probe specificity, we examined the effects of the new TRPML antagonists ML-SI1 and ML-SI3 (Samie et al., 2013). ML-SI1 could not be used because it evoked $Ca^{2+}$ signals (Fig. S1A). ML-SI3, however, inhibited ML-SA1-evoked $Ca^{2+}$ signals (Fig. 1E,F). Collectively, these data suggest that, contrary to the prevailing view, activation of endogenous TRPMLs is capable of evoking global $Ca^{2+}$ signals.

### Agonist-evoked $Ca^{2+}$ signals require TRPML1

To investigate the mechanism underlying agonist-evoked $Ca^{2+}$ signals, we examined the effects of expressing active TRPML1 and inactive TRPML1 mutated within the pore region (TRPML1[D471K]) (Yamaguchi et al., 2011). Confocal analyses of HeLa cells expressing TRPML1 and TRPML1[D471K] revealed a comparable punctate distribution consistent with localisation to lysosomes (Fig. 2A). Accordingly, there was marked colocalisation of both proteins with lysotracker (a fluorescent acidotrope) and LAMP1 (a lysosomal marker) (Fig. 2B–E).

In control experiments, ML-SA1 evoked $Ca^{2+}$ signals in cells expressing LAMP1 (Fig. 3A). The responses were similar to those in un-transfected cells (Fig. 1). In cells expressing TRPML1, however, there was a large potentiation of the $Ca^{2+}$ signal (Fig. 3A) such that essentially all of the cells responded (Fig. 3B,C). The potentiating effect of TRPML1 was specific because it was not observed with TRPML1[D471K] (Fig. 3A–C). Similar results were

obtained in fibroblasts (Fig. S1C,D) although this analysis was more limited due to the difficulty in transfecting these cells. Notably, ML-SA1-evoked $Ca^{2+}$ signals were inhibited in cells expressing TRPML1[D471K] relative to cells expressing LAMP1 (Fig. 3A–C). The inhibitory effect of TRPML1[D471K] is likely due to dominant-negative activity resulting from oligomerisation with endogenous TRPML1 (Venkatachalam et al., 2006).

We also tested the effect of the structurally distinct mucolipin analogue MK6-83. Like ML-SA1, MK6-83 evoked large $Ca^{2+}$ signals in cells expressing TRPML1 but not TRPML1[D471K] (Fig. 3D,E). $Ca^{2+}$ signals evoked by both ML-SA1 and MK6-83 in TRPML1-expressing cells were blocked by ML-SI3 (Fig. 3F–I). These molecular and chemical analyses establish the requirement for TRPML1 in global $Ca^{2+}$ signalling.

### TRPML1 couples lysosomal and ER $Ca^{2+}$ release

To define the $Ca^{2+}$ sources underlying TRPML1-dependent $Ca^{2+}$ signals, we first established the relative contribution of store release and $Ca^{2+}$ entry to the evoked responses. As shown in Fig. 4A,B, removal of extracellular $Ca^{2+}$ reduced the peak response upon ML-SA1 stimulation and eliminated the sustained phase. ML-SA1-evoked $Ca^{2+}$ signals in $Ca^{2+}$-free medium were TRPML1 dependent, as judged by the lack of ML-SA1-evoked $Ca^{2+}$ signals in TRPML1[D471K]-expressing cells and upon treatment with ML-SI3 (Fig. 4C). These data suggest that ML-SA1 evokes both $Ca^{2+}$ release and $Ca^{2+}$ influx.

We used the lysosomotropic agent Gly-Phe β-naphthylamide (GPN) to disrupt lysosomes. This dipeptide causes osmotic destabilisation of lysosomes and other cathepsin-C-positive compartments (Jadot et al., 1984). GPN treatment resulted in a rapid loss of Lysotracker® red fluorescence consistent with its action on lysosomes (Fig. S1E,F) and inhibited the responses to ML-SA1 indicating a requirement for lysosomes in ML-SA1-evoked $Ca^{2+}$ release (Fig. 4D). These data are consistent with the lysosomal localisation of TRPMLs (Fig. 2). However, despite the complete compromise of lysosomes upon GPN treatment, the resulting $Ca^{2+}$ signals were modest relative to those evoked by ML-SA1 (Fig. 4D). This suggested that ML-SA1 did not exclusively release $Ca^{2+}$ from the lysosomes.

We considered the possibility that activation of TRPMLs might be followed by $Ca^{2+}$ release from the ER in a manner similar to activation of TPCs by NAADP (Cancela et al., 1999; Patel et al., 2010). To test this, we examined the effects of ML-SA1 after depleting ER $Ca^{2+}$ stores with thapsigargin. As shown in Fig. 4D, thapsigargin treatment blocked the responses to ML-SA1 indicating a clear requirement for ER $Ca^{2+}$ stores in ML-SA1 action. To further probe the role of the ER, we used 2-APB to block inositol 1,4,5-trisphosphate ($IP_3$) receptors. As shown in Fig. 4D, 2-APB (100 µM) inhibited ML-SA1-evoked responses. A summary of these data is provided in Fig. 4E. We conclude that activation of TRPMLs on lysosomes triggers $Ca^{2+}$ release from the ER.

### TRPML1 mediates $Ca^{2+}$ influx

Finally, we examined the nature of the $Ca^{2+}$ entry pathway evoked by TRPML1 activation. Because store-operated $Ca^{2+}$ entry is a ubiquitous pathway underlying $Ca^{2+}$ influx in non-excitable cells, we tested the effects of the $Ca^{2+}$ entry inhibitor BTP2. BTP2 (20 µM) completely prevented $Ca^{2+}$ signals evoked by $Ca^{2+}$ add-back following depletion of ER $Ca^{2+}$ stores with thapsigargin (Fig. S2A,B). However, BTP2 did not affect the amplitude of $Ca^{2+}$ signals evoked by ML-SA1 (Fig. 5A,B) although it did slow the rate of rise (Fig. S2C). These data suggest that store-operated $Ca^{2+}$ entry
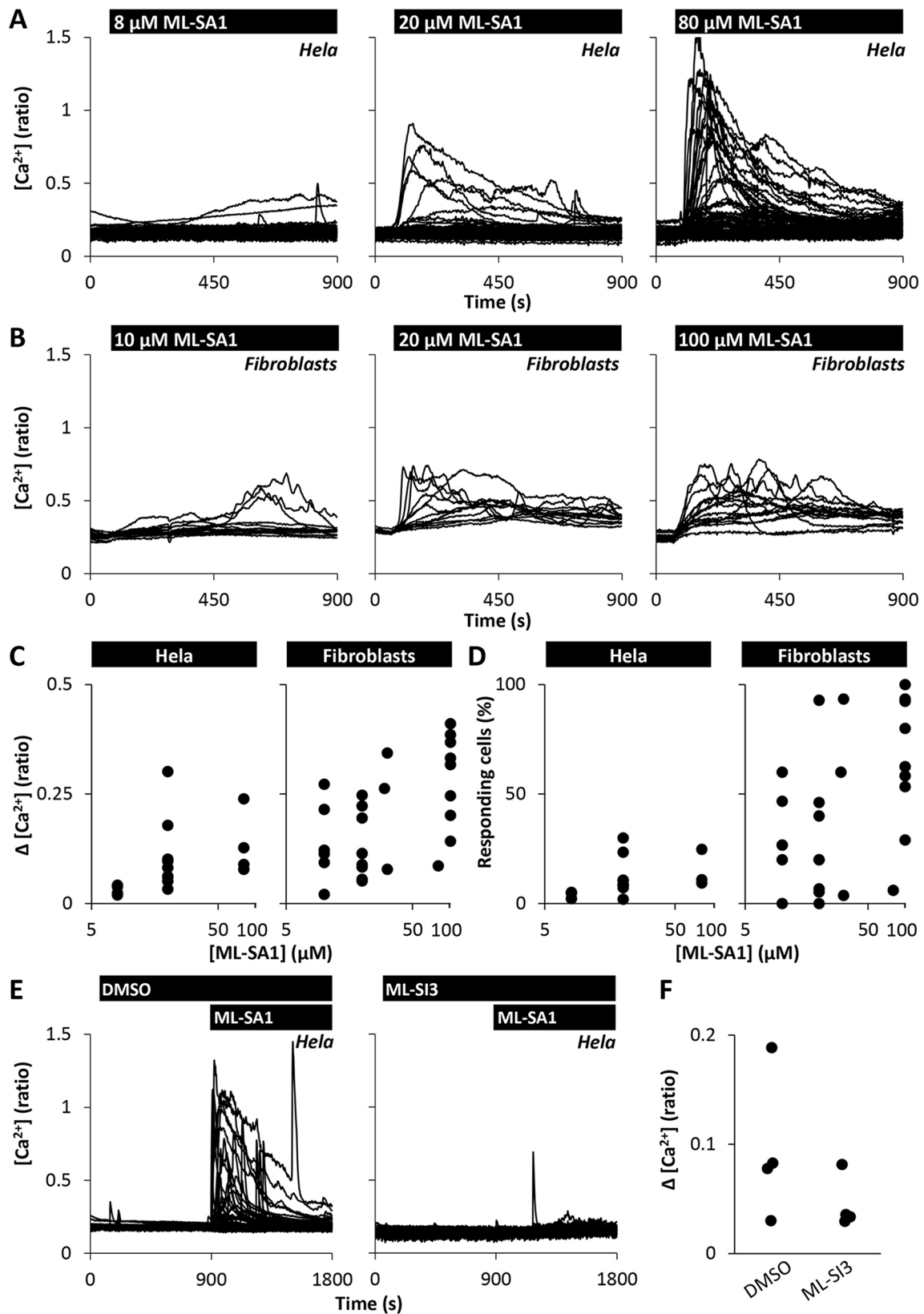
**Fig. 1. The TRP mucolipin agonist ML-SA1 evokes global Ca$^{2+}$ signals.** (A–D) Effect of ML-SA1 on cytosolic Ca$^{2+}$ levels. Cytosolic Ca$^{2+}$ levels of individual Fura-2-loaded HeLa cells (A) or fibroblasts (B) from an exemplar population stimulated with increasing concentrations of ML-SA1. (C,D) Summary data quantifying the peak response (C) and percentage of responsive cells within the population (D). Each data point represents an independent repetition. A total of 350–788 HeLa cells and 81–140 fibroblasts were analysed. (E,F) Effect of the mucolipin inhibitor ML-SI3 on agonist-evoked Ca$^{2+}$ signals. (E) Cytosolic Ca$^{2+}$ levels of HeLa cells stimulated with 20 μM ML-SA1 in the presence of vehicle (0.1% DMSO) or 10 μM ML-SI3. (F) Summary data for the experiments in E (366–406 cells).
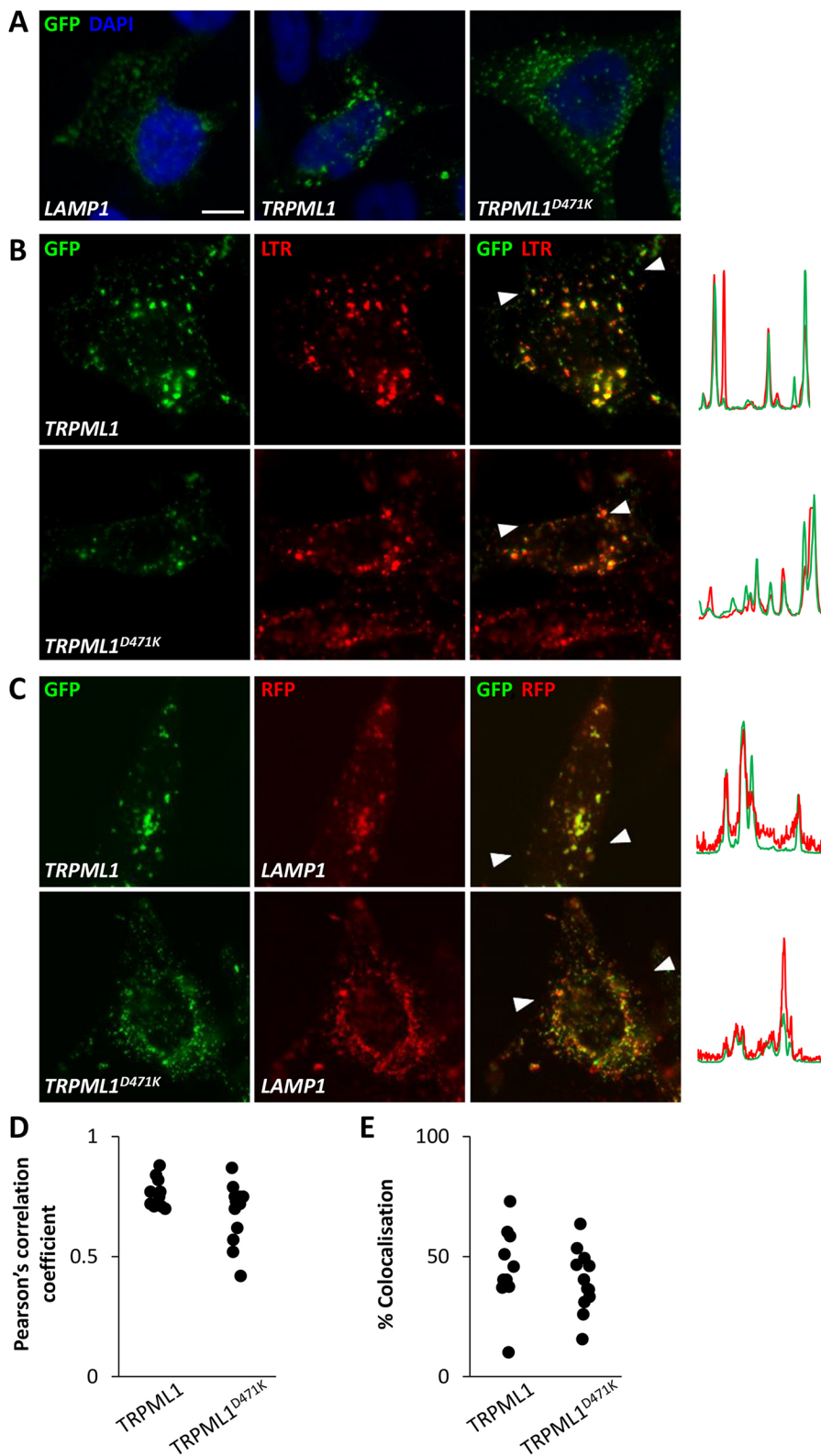
**Fig. 2. Subcellular distribution of TRPML1.**
(A) Confocal fluorescence images (green) of fixed HeLa cells expressing GFP-tagged LAMP1 (left), TRPML1 (middle) or TRPML1$^{D471K}$ (right). Nuclei were stained using DAPI (blue). (B,C) Confocal fluorescence images of cells expressing GFP–TRPML1 or GFP–TRPML1$^{D471K}$ and either colabelled with Lysotracker® Red (LTR) and imaged live (B) or co-transfected with LAMP1-mRFP and imaged following fixation (C). Overlays of images are shown in the right panels where arrows delineate the regions from which red–green intensity plots were derived. Scale bar: 10 µm. (D,E) Summary data of experiments in C quantifying Pearson's correlation coefficients (D) and the percentage of vesicles showing colocalisation (E). Each point represents an individual cell from two independent transfections.

does not play a major role in Ca$^{2+}$ signals evoked by TRPML1 activation.

The above data raised the possibility that TRPML1 might mediate Ca$^{2+}$ entry more directly. To test this, we examined the effects of ML-SA1 on Fe$^{2+}$ entry. Fe$^{2+}$ permeates TRPML1 and, like several other metal ions, quenches Fura-2 fluorescence (Dong et al., 2008). Fura-2-

loaded HeLa cells were therefore challenged with FeCl$_2$ (1 mM) in nominally Ca$^{2+}$-free medium after stimulation with ML-SA1. FeCl$_2$ induced a significant quench of Fura-2 fluorescence in cells expressing TRPML1 (Fig. 5C). This effect was blocked by ML-SI3 (Fig. 5C,D) and was not observed in cells expressing TRPML1$^{D471K}$ (Fig. 5G,H). Similar results were obtained upon stimulation with
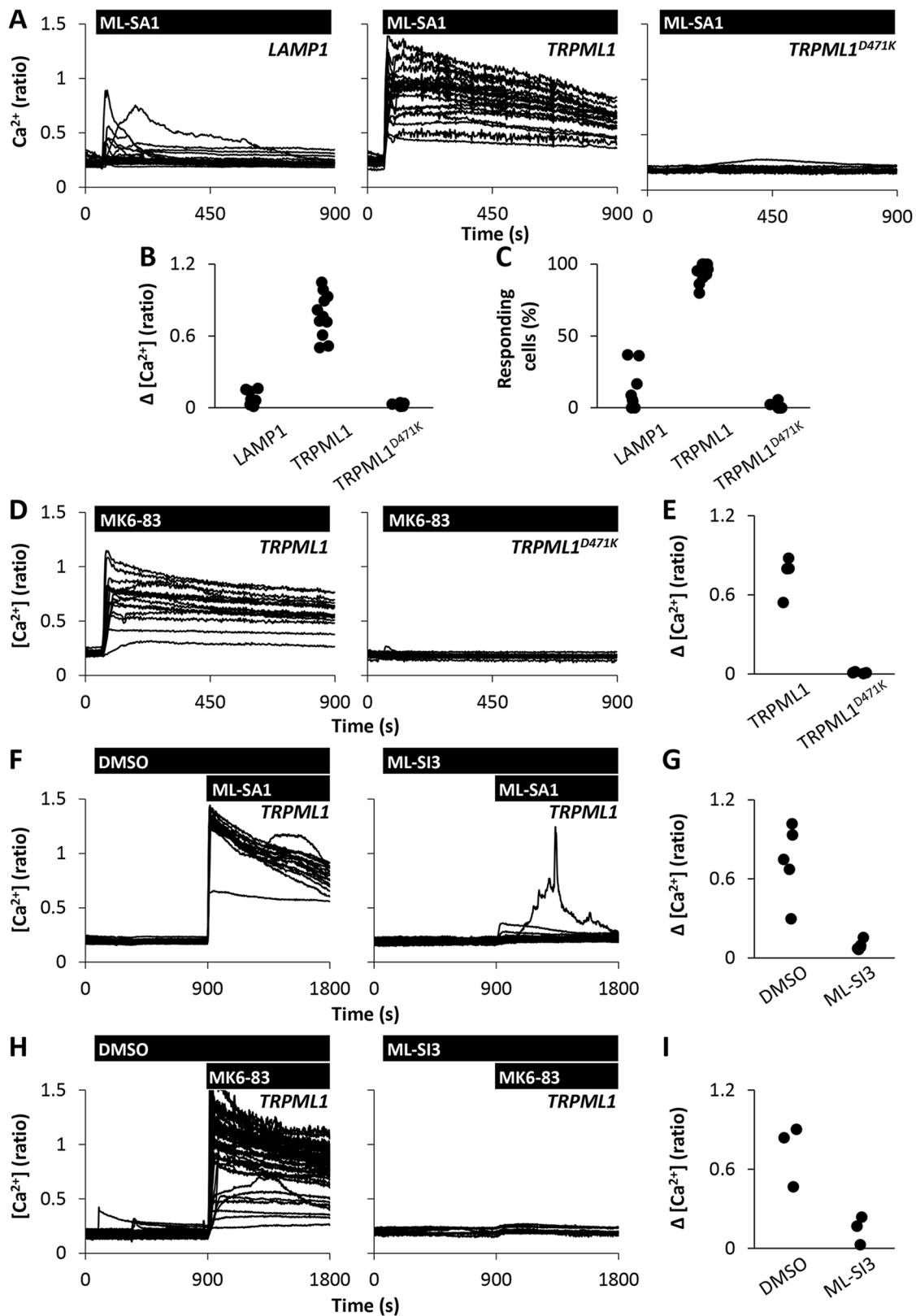
**Fig. 3. Agonist-evoked Ca²⁺ signals require TRPML1.** (A–C) Effect of TRPML expression on ML-SA1-evoked Ca²⁺ signals. (A) Cytosolic Ca²⁺ levels of individual LAMP1, TRPML1- or TRPML1^D471K-expressing HeLa cells stimulated with 20 μM ML-SA1. (B,C) Summary data of experiments in A where each data point represents an independent repetition. The total number of cells analysed was 193–367. (D,E) Effect of TRPML expression on MK6-83-evoked Ca²⁺ signals. (D) Cytosolic Ca²⁺ levels of individual TRPML1- or TRPML1^D471K-expressing HeLa cells stimulated with 20 μM MK6-83. (E) Summary data of experiments in D (111–128 cells). (F–I) Effect of ML-SI3 on agonist-evoked Ca²⁺ signals. Cytosolic Ca²⁺ levels of individual TRPML1-expressing HeLa cells stimulated with 20 μM ML-SA1 (F) or 20 μM MK6-83 (H) in the presence of vehicle (0.1% DMSO) or 10 μM ML-SI3. Summary data are shown in panels (G; 120 cells) and (I; 101–107 cells), respectively.
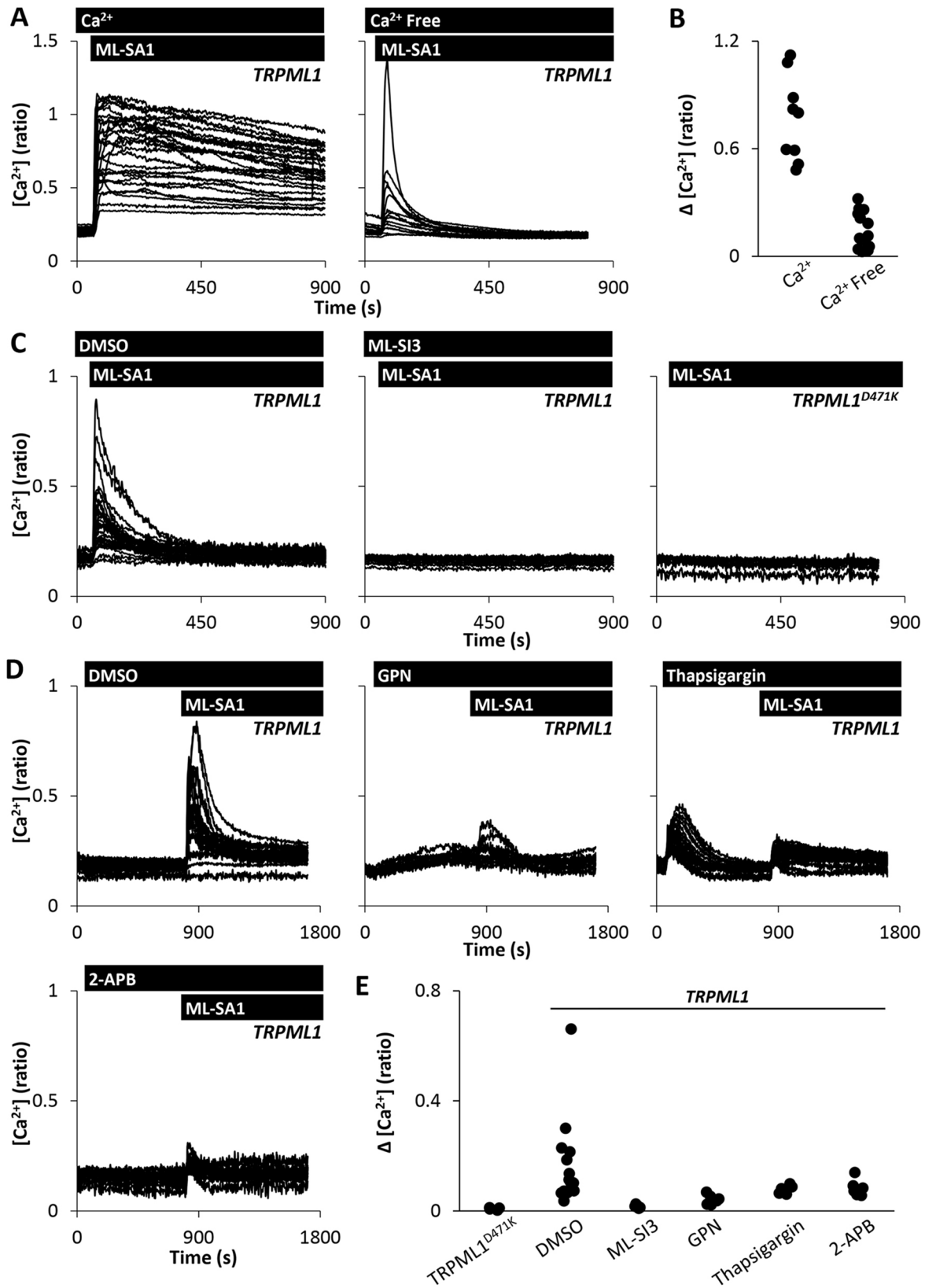
Fig. 4. TRPML1 couples lysosomal and ER Ca²⁺ release. (A,B) Effect of extracellular Ca²⁺ on agonist-evoked Ca²⁺ responses. (A) Cytosolic Ca²⁺ levels of TRPML1-expressing HeLa cells stimulated with 20 μM ML-SA1 in Ca²⁺-containing or Ca²⁺-free Hepes-buffered saline. (B) Summary data of experiments in A where each data point represents an independent repetition. The total number of cells analysed was 184–284. (C) Cytosolic Ca²⁺ levels of TRPML1 or TRPML1$^{D471K}$-expressing HeLa cells stimulated with 20 μM ML-SA1 with or without 10 μM ML-SI3 in Ca²⁺-free medium. (D,E) Effect of disrupting Ca²⁺ stores on agonist-evoked Ca²⁺ responses. (D) Cytosolic Ca²⁺ levels of TRPML1-expressing HeLa cells stimulated with 20 μM ML-SA1 following pre-treatment with DMSO, 200 μM GPN, 1 μM thapsigargin or 100 μM 2-APB. (E) Summary data of experiments in D (71–462 cells). Experiments were performed in Ca²⁺-free medium.
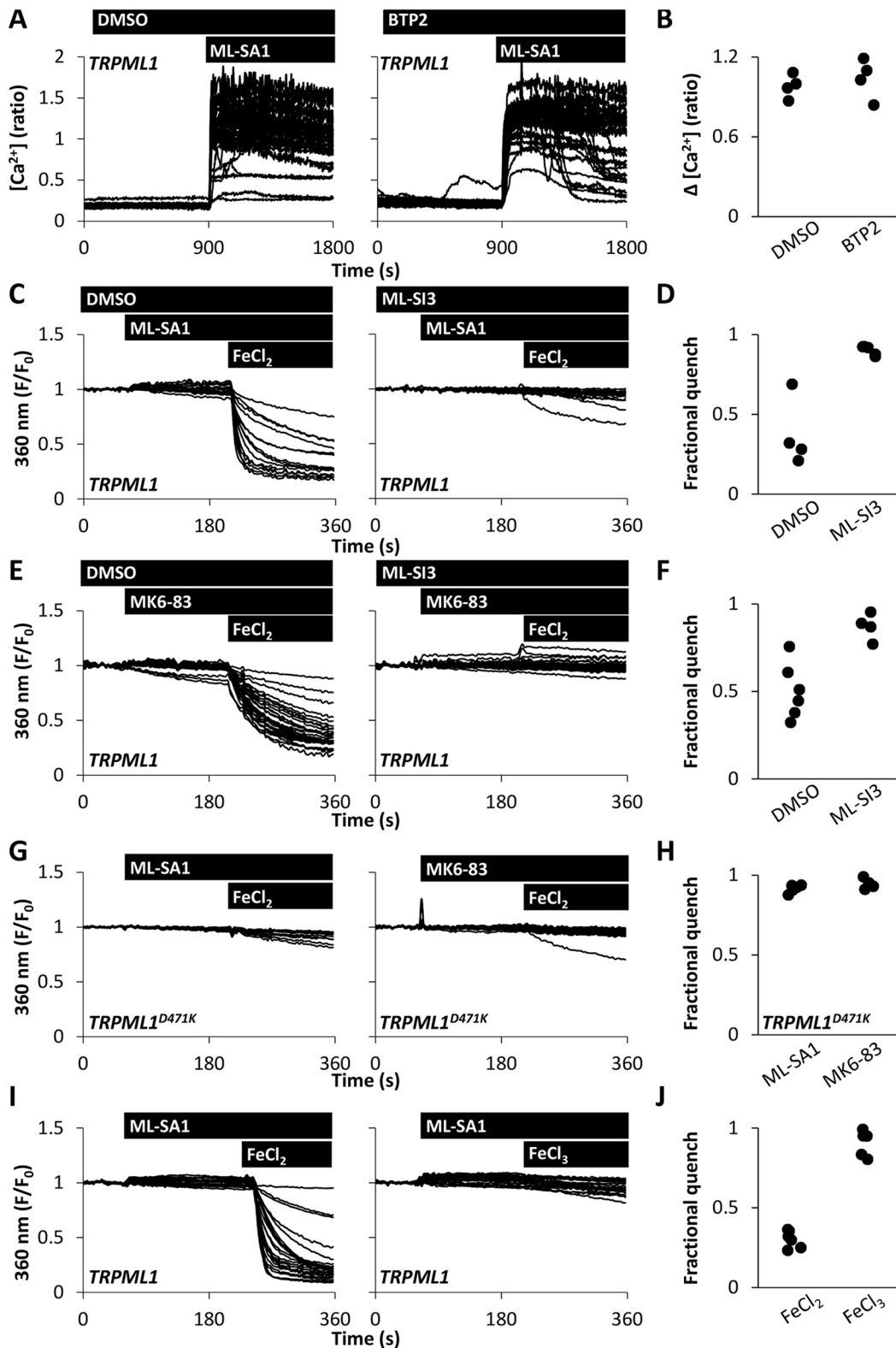
**Fig. 5. TRPML1 mediates Ca$^{2+}$ influx.** (A,B) Effect of blocking store-operated Ca$^{2+}$ influx on agonist-evoked Ca$^{2+}$ responses. (A) Cytosolic Ca$^{2+}$ levels of TRPML1-expressing HeLa cells stimulated with 20 µM ML-SA1 in the presence of vehicle (0.1% DMSO) or 20 µM BTP2. (B) Summary data of experiments in A where each data point represents an independent repetition. The total number of cells analysed was 151–173. (C–J) Effect of TRPML1 activation on Fe ion entry. HeLa cells expressing TRPML1 were stimulated with 20 µM ML-SA1 (C) or MK6-83 (E) and then 1 mM FeCl$_2$ in the presence of vehicle (0.1% DMSO) or 10 µM ML-SI3. HeLa cells expressing TRPML1$^{D471K}$ were stimulated with either 20 µM ML-SA1 or MK6-83 (G). HeLa cells expressing TRPML1 were stimulated with 20 µM ML-SA1 and either 1 mM FeCl$_2$ or 1 mM FeCl$_3$ (I). Experiments were performed in nominally Ca$^{2+}$-free medium. Fluorescence signals (denoted F) were recorded after excitation at the isosbestic wavelength of Fura-2 (360 nm) and normalised to that at the beginning of recording (denoted F$_0$). Summary data (D,F,H, J; for C,E,G and I, respectively) quantifying the fractional loss of fluorescence 144s after addition of Fe$^{2+}$ or Fe$^{3+}$ under the various conditions (80–169 cells).

MK6-83 (Fig. 5E–H). Challenge with $FeCl_3$ (1 mM) after stimulation with ML-SA1 was without effect (Fig. 5I,J) attesting to specificity. BTP2 slowed $Fe^{2+}$ entry (Fig. S2D,E), however, add-back of $Fe^{2+}$ following depletion of $Ca^{2+}$ stores with thapsigargin did not result in a significant quench (Fig. S2F,G).

Collectively, these data provide evidence that TRPML1 supports divalent cation entry across the plasma membrane.

## DISCUSSION

In this study, we have shown that activation of TRPMLs by two structurally distinct agonists, in both a human cell line and primary cultures, evokes global $Ca^{2+}$ signals. These data indicate that TRPMLs do not solely mediate local $Ca^{2+}$ release events from endo-lysosomal compartments. Indeed, we provide evidence that activation of TRPMLs can evoke both $Ca^{2+}$ release and $Ca^{2+}$ entry.

We have dissected global $Ca^{2+}$ release signals into both lysosomal and ER components. There is much evidence supporting the transmission of $Ca^{2+}$ signals from endo-lysosomes to the ER but to date such 'chatter' has been ascribed exclusively to the actions of NAADP and TPCs (Patel and Brailoiu, 2012). Our study extends such coupling to TRPMLs, raising the possibility that other $Ca^{2+}$-permeable endo-lysosomal channels such as P2X4 receptors and TRPM2 might also functionally couple to ER $Ca^{2+}$ release channels (Patel and Cai, 2015).

Inhibition of TRPML1 by plasma membrane $PI(4,5)P_2$ is thought to ensure channel activation only in endo-lysosomal compartments (Zhang et al., 2012). In accordance with this idea, basal (unstimulated) whole-cell currents are not detectable in TRPML1-expressing cells. SF-51 (Grimm et al., 2010), the precursor to ML-SA1, however, has been reported to mediate a TRPML1 plasma membrane current (Zhang et al., 2012) consistent with our $Ca^{2+}$ and $Fe^{2+}$ entry measurements. Divalent cation entry might therefore result from targeting of a small fraction of TRPML1 to the plasma membrane. Although blockade of store-operated channels reduced TRPML1-dependent $Ca^{2+}$ and $Fe^{2+}$ entry (albeit modestly), the amplitude of the $Ca^{2+}$ signal upon maximal $Ca^{2+}$ ER store depletion was substantially smaller than that evoked by agonist activation. Indeed, store-operated $Fe^{2+}$ entry was not demonstrable under our conditions. These data raise the possibility that BTP2 might directly inhibit TRPML1 similar to its effects on TRP-canonical (TRPC) channels (He et al., 2005).

The multi-compartment actions of TRPML1 offer fresh perspective on interpreting $Ca^{2+}$ signals recorded using $Ca^{2+}$ reporters fused to TRPML1 (Bae et al., 2014; Cao et al., 2015; Medina et al., 2015; Shen et al., 2012). We suggest that such signals might additionally reflect $Ca^{2+}$ release from the ER and $Ca^{2+}$ entry. Indeed, defects in $Ca^{2+}$ signals reported using such indicators in scenarios of TRPML1 dysfunction are perplexing given that expression of TRPML1 is able to rescue phenotypic defects such as lysosomal storage (Cao et al., 2015; Shen et al., 2012). Use of inert lysosomal proteins for targeting (McCue et al., 2013) and/or low-affinity $Ca^{2+}$ indicators, to better insulate against bulk cytosolic $Ca^{2+}$ changes, might aid in isolating local lysosomal $Ca^{2+}$ release events. Finally, how TRPMLs are endogenously activated remains to be established, but $PI(3,5)P_2$ is a clear candidate raising the possibility that changes in its levels in response to cues such as growth factors might regulate global $Ca^{2+}$ dynamics.

## MATERIALS AND METHODS
### Cell culture
HeLa cells and primary cultured human skin fibroblasts from healthy individuals (Kilpatrick et al., 2013) were maintained in Dulbecco's modified Eagle's medium (DMEM) supplemented with 10% (v/v) fetal bovine serum, 100 units/ml penicillin and 100 µg/ml streptomycin (all from Invitrogen) at 37°C in a humidified atmosphere with 5% $CO_2$. Cells were passaged using trypsin (HeLa) or scraping (fibroblasts) and plated onto 13-mm glass coverslips prior to microscopy. For HeLa cells, coverslips were coated with poly-L-lysine (Sigma). Cells were transfected with plasmids using Lipofectamine 2000 according to the manufacturer's instructions. Plasmids encoding the following proteins were described previously: C-terminally GFP-tagged LAMP1 (Falcón-Pérez et al., 2005), C-terminally mRFP-tagged LAMP1 (Sherer et al., 2003) and N-terminally GFP-tagged wild-type or D471K human TRPML1 (Yamaguchi et al., 2011).

### Cell labelling
All live imaging experiments were performed in HEPES-buffered saline (HBS) comprising (in mM): 1.25 $KH_2PO_4$, 2 $CaCl_2$, 2 $MgSO_4$, 3 KCl, 156 NaCl, 10 glucose, and 10 HEPES (pH 7.4; all from Sigma). For measurement of cytosolic $Ca^{2+}$ concentration and $Fe^{2+}$ or $Fe^{3+}$ entry, cells were incubated with Fura-2 AM (2.5 µM) and 0.005% v/v pluronic acid (from Invitrogen) for 1 h. For measurement of lysosome distribution, cells were incubated with Lysotracker® Red (100 nM) (Invitrogen) for 15 min. After labelling, cells were washed with HBS and mounted in a 1-ml imaging chamber (Biosciences Tools) prior to microscopy. For measurement of colocalisation, cells were co-transfected with GFP–TRPML1 or GFP–TRPML1$^{D471K}$ together with LAMP1–mRFP and fixed with 4% paraformaldehyde prior to confocal microscopy. For visualisation of nuclei, cells were incubated with 1 µg/ml DAPI for 5 min.

### Epifluorescence microscopy
Epifluorescence images were captured every 3 s with a cooled coupled device camera (TILL photonics) attached to an Olympus IX71 inverted fluorescence microscope fitted with a 20× objective, and a monochromator light source. Fura-2 was excited at 340, 360 or 380 nm, and Lysotracker® Red at 560 nm. Emitted fluorescence was captured using a 440-nm long-pass filter (Fura-2) and 590-nm filter (Lysotracker® Red). TRPML1-expressing cells were identified by monitoring fluorescence of GFP (excitation 488 nm, emission 505 nm). Cells were stimulated with ML-SA1, GW405833 hydrochloride (Sigma; also known as ML-SI1, Haoxing Xu, Department of Molecular, Cellular, and Developmental Biology, University of Michigan, USA, personal communication), ML-SI3 (a kind gift from Haoxing Xu), MK6-83 synthesised as described previously (Chen et al., 2014), GPN (Santa Cruz Biotechnology), BTP2 (Sigma), thapsigargin (Merck), 2-aminoethoxydiphenyl borate (2-APB, Sigma). Where indicated, $Ca^{2+}$ was omitted from the HBS (nominally $Ca^{2+}$-free) or replaced with 1 mM EGTA ($Ca^{2+}$-free). For $Fe^{2+}$ or $Fe^{3+}$ quench experiments, cells were stimulated using freshly prepared 100 mM stock solutions of either $FeCl_2$ or $FeCl_3$ (Sigma). The maximal fluorescence ratio change ($Ca^{2+}$) or the fractional quench at 360 nm excitation ($Fe^{2+}$ or $Fe^{3+}$) were quantified on an individual cell basis and averaged for all cells in a given field of view. Experiments were repeated at least three times and all individual data points plotted. The total number of cells analysed is stated in the legends.

### Confocal microscopy
Confocal images were captured using an LSM510 confocal scanner (Zeiss) attached to a Zeiss Axiovert 200M inverted microscope fitted with a 63× Plan Apochromat water-immersion objective. DAPI, GFP and Lysotracker® Red or mRFP were excited at 364 nm, 488 nm and 543 nm, and emitted fluorescence was captured using 385–470 nm, 505–550 nm and 560–615 nm band-pass filters, respectively. Pearson's correlation coefficients were calculated from z-stacks (1-µm intervals, 8–12 slices) using the ImageJ plugin Coloc2. The fraction of colocalised vesicles was calculated from the middle slice or slices using the ImageJ plugin SQUASSH.

### Competing interests
The authors declare no competing or financial interests.

## References
Bae, M., Patel, N., Xu, H., Lee, M., Tominaga-Yamanaka, K., Nath, A., Geiger, J., Gorospe, M., Mattson, M. P. and Haughey, N. J. (2014). Activation of TRPML1 clears intraneuronal Aβ in preclinical models of HIV infection. *J. Neurosci.* **34**, 11485-11503.

Bargal, R., Avidan, N., Ben-Asher, E., Olender, Z., Zeigler, M., Frumkin, A., Raas-Rothschild, A., Glusman, G., Lancet, D. and Bach, G. (2000). Identification of the gene causing mucolipidosis type IV. *Nat. Genet.* **26**, 118-123.

Berridge, M. J., Bootman, M. D. and Roderick, H. L. (2003). Calcium signalling: dynamics, homeostasis and remodelling. *Nat. Rev. Mol. Cell Biol.* **4**, 517-529.

Brailoiu, E., Churamani, D., Cai, X., Schrlau, M. G., Brailoiu, G. C., Gao, X., Hooper, R., Boulware, M. J., Dun, N. J., Marchant, J. S. et al. (2009). Essential requirement for two-pore channel 1 in NAADP-mediated calcium signaling. *J. Cell Biol.* **186**, 201-209.

Calcraft, P. J., Ruas, M., Pan, Z., Cheng, X., Arredouani, A., Hao, X., Tang, J., Rietdorf, K., Teboul, L., Chuang, K.-T. et al. (2009). NAADP mobilizes calcium from acidic organelles through two-pore channels. *Nature* **459**, 596-600.

Cancela, J. M., Churchill, G. C. and Galione, A. (1999). Coordination of agonist-induced Ca²⁺-signalling patterns by NAADP in pancreatic acinar cells. *Nature* **398**, 74-76.

Cao, Q., Zhong, X. Z., Zou, Y., Zhang, Z., Toro, L. and Dong, X. P. (2015). BK channels alleviate lysosomal storage diseases by providing positive feedback regulation of lysosomal Ca²⁺ release. *Dev. Cell* **33**, 427-441.

Chen, C. C., Keller, M., Hess, M., Schiffmann, R., Urban, N., Wolfgardt, A., Schaefer, M., Bracher, F., Biel, M., Wahl-Schott, C. et al. (2014). A small molecule restores function to TRPML1 mutant isoforms responsible for mucolipidosis type IV. *Nat. Commun.* **5**, 4681.

Christensen, K. A., Myers, J. T. and Swanson, J. A. (2002). pH-dependent regulation of lysosomal calcium in macrophages. *J. Cell Sci.* **115**, 599-607.

Clapham, D. E. (2007). Calcium signaling. *Cell* **131**, 1047-1058.

Dong, X.-P., Cheng, X., Mills, E., Delling, M., Wang, F., Kurz, T. and Xu, H. (2008). The type IV mucolipidosis-associated protein TRPML1 is an endolysosomal iron release channel. *Nature* **455**, 992-996.

Dong, X. P., Shen, D., Wang, X., Dawson, T., Li, X., Zhang, Q., Cheng, X., Zhang, Y., Weisman, L. S., Delling, M. et al. (2010). PI(3,5)P₂ controls membrane traffic by direct activation of mucolipin Ca²⁺ release channels in the endolysosome. *Nat. Commun.* **1**, 38.

Falcón-Pérez, J. M., Nazarian, R., Sabatti, C. and Dell'Angelica, E. C. (2005). Distribution and dynamics of Lamp1-containing endocytic organelles in fibroblasts deficient in BLOC-3. *J. Cell Sci.* **118**, 5243-5255.

Galione, A. (2015). A primer of NAADP-mediated Ca²⁺ signalling: from sea urchin eggs to mammalian cells. *Cell Calcium* **58**, 27-47.

García-Añoveros, J. and Wiwatpanit, T. (2014). TRPML2 and mucolipin evolution. *Handb. Exp. Pharmacol.* **222**, 647-658.

Grimm, C., Cuajungco, M. P., van Aken, A. F., Schnee, M., Jors, S., Kros, C. J., Ricci, A. J. and Heller, S. (2007). A helix-breaking mutation in TRPML3 leads to constitutive activity underlying deafness in the varitint-waddler mouse. *Proc. Natl. Acad. Sci. USA* **104**, 19583-19588.

Grimm, C., Jörs, S., Saldanha, S. A., Obukhov, A. G., Pan, B., Oshima, K., Cuajungco, M. P., Chase, P., Hodder, P. and Heller, S. (2010). Small molecule activators of TRPML3. *Chem. Biol.* **17**, 135-148.

Grimm, C., Hassan, S., Wahl-Schott, C. and Biel, M. (2012). Role of TRPML and two-pore channels in endo-lysosomal cation homeostasis. *J. Pharmacol. Exp. Ther.* **342**, 236-244.

He, L.-P., Hewavitharana, T., Soboloff, J., Spassova, M. A. and Gill, D. L. (2005). A functional link between store-operated and TRPC channels revealed by the 3,5-bis(trifluoromethyl)pyrazole derivative, BTP2. *J. Biol. Chem.* **280**, 10997-11006.

Hockey, L. N., Kilpatrick, B. S., Eden, E. R., Lin-Moshier, Y., Brailoiu, G. C., Brailoiu, E., Futter, C., Schapira, A. H., Marchant, J. S. and Patel, S. (2015). Dysregulation of lysosomal morphology by pathogenic LRRK2 is corrected by TPC2 inhibition. *J. Cell Sci.* **128**, 232-238.

Jadot, M., Colmant, C., Wattiaux-De Coninck, S. and Wattiaux, R. (1984). Intralysosomal hydrolysis of glycyl-L-phenylalanine 2-naphthylamide. *Biochem. J.* **219**, 965-970.

Kilpatrick, B. S., Eden, E. R., Schapira, A. H., Futter, C. E. and Patel, S. (2013). Direct mobilisation of lysosomal Ca²⁺ triggers complex Ca²⁺ signals. *J. Cell Sci.* **126**, 60-66.

Kim, H. J., Li, Q., Tjon-Kon-Sang, S., So, I., Kiselyov, K. and Muallem, S. (2007). Gain-of-function mutation in TRPML3 causes the mouse Varitint-Waddler phenotype. *J. Biol. Chem.* **282**, 36138-36142.

Kiselyov, K. K., Ahuja, M., Rybalchenko, V., Patel, S. and Muallem, S. (2012). The intracellular Ca²⁺ channels of membrane traffic. *Channels (Austin).* **6**, 344-351.

Lee, J.-H., McBrayer, M. K., Wolfe, D. M., Haslett, L. J., Kumar, A., Sato, Y., Lie, P. P. Y., Mohan, P., Coffey, E. E., Kompella, U. et al. (2015). Presenilin 1 maintains lysosomal Ca²⁺ homeostasis via TRPML1 by regulating vATPase-mediated lysosome acidification. *Cell Rep.* **12**, 1430-1444.

Lloyd-Evans, E., Morgan, A. J., He, X., Smith, D. A., Elliot-Smith, E., Sillence, D. J., Churchill, G. C., Schuchman, E. H., Galione, A. and Platt, F. M. (2008). Niemann-Pick disease type C1 is a sphingosine storage disease that causes deregulation of lysosomal calcium. *Nat. Med.* **14**, 1247-1255.

McCue, H. V., Wardyn, J. D., Burgoyne, R. D. and Haynes, L. P. (2013). Generation and characterization of a lysosomally targeted, genetically encoded Ca²⁺-sensor. *Biochem. J.* **449**, 449-457.

Medina, D. L., Di Paola, S., Peluso, I., Armani, A., De Stefani, D., Venditti, R., Montefusco, S., Scotto-Rosato, A., Prezioso, C., Forrester, A. et al. (2015). Lysosomal calcium signalling regulates autophagy through calcineurin and TFEB. *Nat. Cell Biol.* **17**, 288-299.

Melchionda, M., Pittman, J. K., Mayor, R. and Patel, S. (2016). Ca²⁺/H⁺ exchange by acidic organelles regulates cell migration in vivo. *J. Cell Biol.* **212**, 803-813.

Park, S., Ahuja, M., Kim, M. S., Brailoiu, G. C., Jha, A., Zeng, M., Baydyuk, M., Wu, L.-G., Wassif, C. A., Porter, F. D. et al. (2016). Fusion of lysosomes with secretory organelles leads to uncontrolled exocytosis in the lysosomal storage disease mucolipidosis type IV. *EMBO Rep.* **17**, 266-278.

Patel, S. (2015). Function and dysfunction of two-pore channels. *Sci. Signal.* **8**, re7.

Patel, S. and Brailoiu, E. (2012). Triggering of Ca²⁺ signals by NAADP-gated two-pore channels: a role for membrane contact sites? *Biochem. Soc. Trans.* **40**, 153-157.

Patel, S. and Cai, X. (2015). Evolution of acid Ca²⁺ stores and their resident Ca²⁺-permeable channels. *Cell Calcium* **57**, 222-230.

Patel, S. and Muallem, S. (2011). Acidic Ca²⁺ stores come to the fore. *Cell Calcium* **50**, 109-112.

Patel, S., Marchant, J. S. and Brailoiu, E. (2010). Two-pore channels: Regulation by NAADP and customized roles in triggering calcium signals. *Cell Calcium* **47**, 480-490.

Penny, C. J., Kilpatrick, B. S., Han, J. M., Sneyd, J. and Patel, S. (2014). A computational model of lysosome-ER Ca²⁺ microdomains. *J. Cell Sci.* **127**, 2934-2943.

Prakriya, M. and Lewis, R. S. (2015). Store-operated calcium channels. *Physiol. Rev.* **95**, 1383-1436.

Pryor, P. R., Mullock, B. M., Bright, N. A., Gray, S. R. and Luzio, J. P. (2000). The role of intraorganellar Ca²⁺ in late endosome–lysosome heterotypic fusion and in the reformation of lysosomes from hybrid organelles. *J. Cell Biol.* **149**, 1053-1062.

Samie, M., Wang, X., Zhang, X., Goschka, A., Li, X., Cheng, X., Gregg, E., Azar, M., Zhuo, Y., Garrity, A. G. et al. (2013). A TRP channel in the lysosome regulates large particle phagocytosis via focal exocytosis. *Dev. Cell* **26**, 511-524.

Shen, D., Wang, X., Li, X., Zhang, X., Yao, Z., Dibble, S., Dong, X.-P., Yu, T., Lieberman, A. P., Showalter, H. D. et al. (2012). Lipid storage disorders block lysosomal trafficking by inhibiting a TRP channel and lysosomal calcium release. *Nat. Commun.* **3**, 731.

Sherer, N. M., Lehmann, M. J., Jimenez-Soto, L. F., Ingmundson, A., Horner, S. M., Cicchetti, G., Allen, P. G., Pypaert, M., Cunningham, J. M. and Mothes, W. (2003). Visualization of retroviral replication in living cells reveals budding into multivesicular bodies. *Traffic* **4**, 785-801.

Venkatachalam, K., Hofmann, T. and Montell, C. (2006). Lysosomal localization of TRPML3 depends on TRPML2 and the mucolipidosis-associated protein TRPML1. *J. Biol. Chem.* **281**, 17517-17527.

Vergarajauregui, S. and Puertollano, R. (2006). Two di-leucine motifs regulate trafficking of mucolipin-1 to lysosomes. *Traffic* **7**, 337-353.

Waller-Evans, H. and Lloyd-Evans, E. (2015). Regulation of TRPML1 function. *Biochem. Soc. Trans.* **43**, 442-446.

Yamaguchi, S., Jha, Y., Li, Q., Soyombo, A. A., Dickinson, G. D., Churamani, D., Brailoiu, E., Patel, S. and Muallem, S. (2011). Transient receptor potential mucolipin 1 (TRPML1) and two-pore channels are functionally independent organellar ion channels. *J. Biol. Chem.* **286**, 22934-22942.

Zhang, F., Xu, M., Han, W.-Q. and Li, P.-L. (2011). Reconstitution of lysosomal NAADP-TRP-ML1 signaling pathway and its function in TRP-ML1⁻/⁻ cells. *Am. J. Physiol. Cell Physiol.* **301**, C421-C430.

Zhang, X., Li, X. and Xu, H. (2012). Phosphoinositide isoforms determine compartment-specific ion channel activity. *Proc. Natl. Acad. Sci. USA* **109**, 11384-11389.
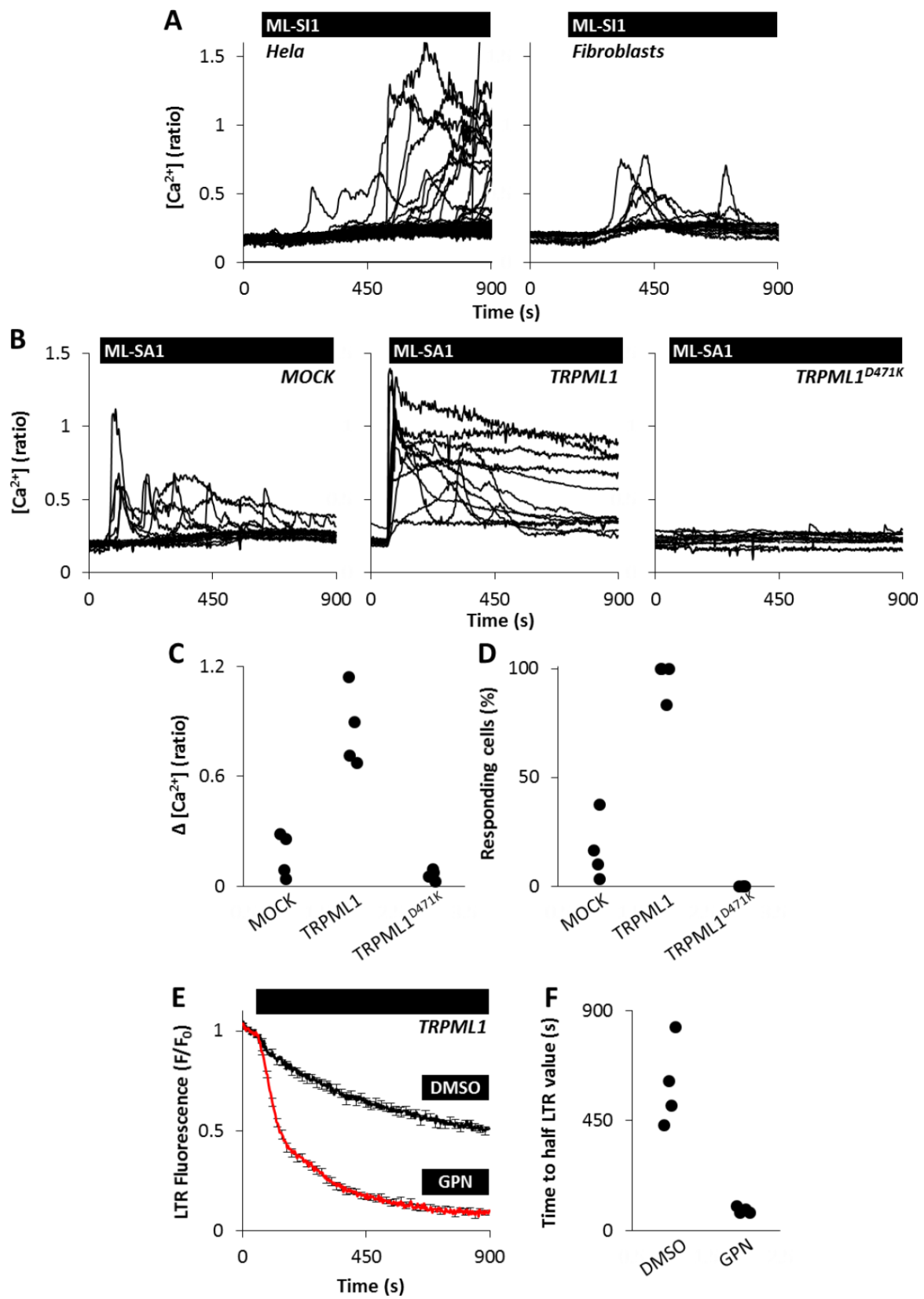
**Figure S1**. (A) The mucolipin inhibitor, ML-SI1 elevates cytosolic $Ca^{2+}$ levels. Cytosolic $Ca^{2+}$ levels of Hela cells and fibroblasts stimulated with 20 µM ML-SI1. (B-D) Agonist-evoked $Ca^{2+}$ signals require TRPML1. (C) Cytosolic $Ca^{2+}$ levels of individual mock transfected fibroblasts or fibroblasts expressing TRPML1 or TRPML1$^{D471K}$ stimulated with 20 µM ML-SA1. (C-D) Summary data (12-97 cells). (E-F) GPN compromises lysosome integrity. (E) Lysotracker$^{®}$ red fluorescence levels of TRPML1 expressing Hela cells stimulated with vehicle (0.1 % DMSO) or 200µM GPN. (F) Summary data quantifying the time taken to achieve half-maximal loss of fluorescence (87-108 cells).
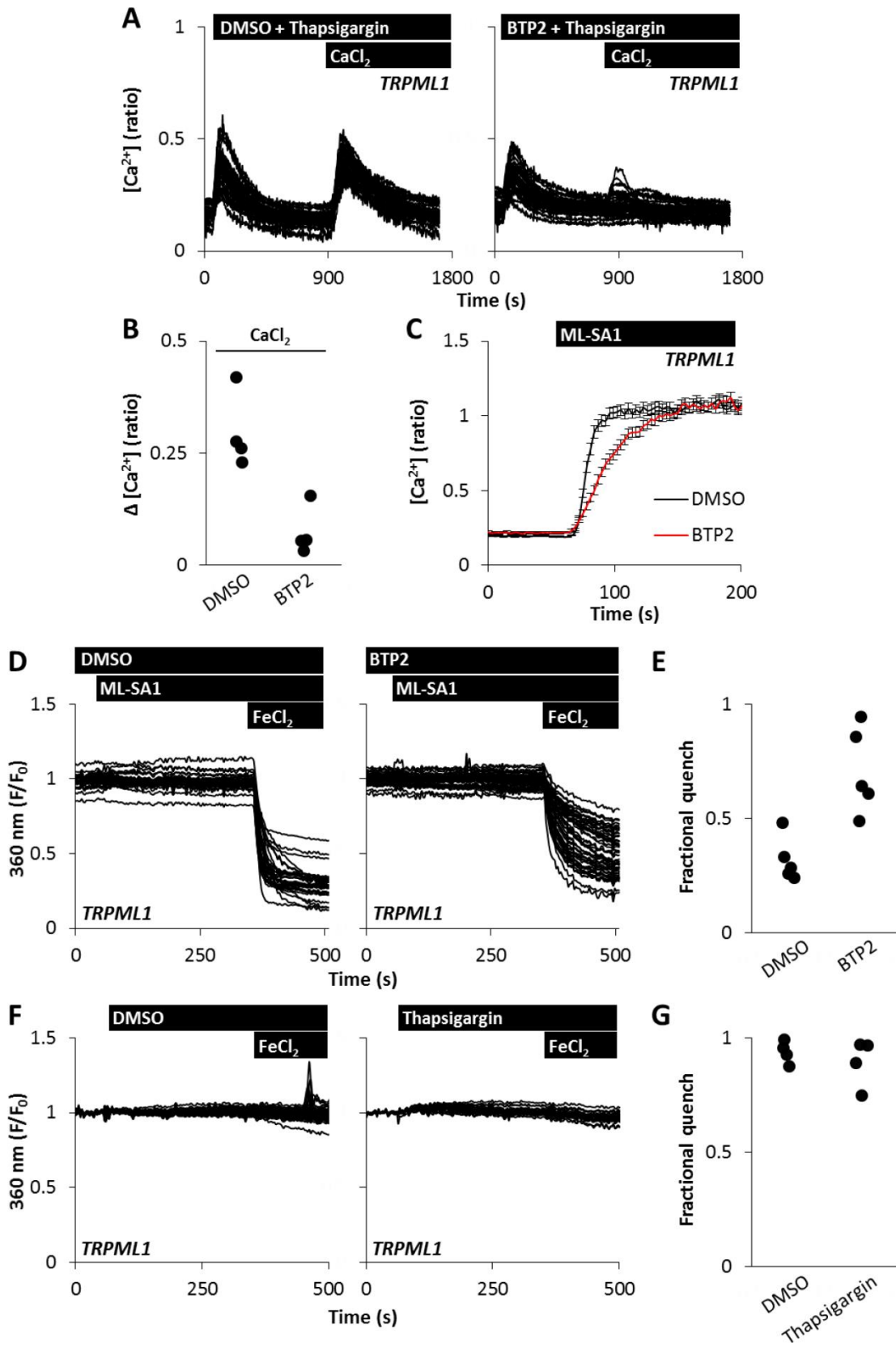
**Figure S2.** (A-B) BTP2 inhibits store-operated $Ca^{2+}$ entry. (A) Cytosolic $Ca^{2+}$ levels of TRPML1-expressing Hela cells in nominally $Ca^{2+}$-free medium sequentially stimulated with 1 μM thapsigargin and 2mM $CaCl_2$ in the presence of vehicle (0.1 % DMSO) or 20 μM BTP2. (B) Summary data (111-117 cells). (C). BTP2 slows ML-SA1–evoked $Ca^{2+}$ signals. Cytosolic $Ca^{2+}$ levels of TRPML1-expressing Hela cells (presented as mean +/- s.e.m. of 120-121 cells, n=3) stimulated with 20 μM ML-SA1 in the presence of vehicle (0.1 % DMSO) or 20 μM BTP2. (D-E) BTP2 slows ML-SA1–evoked $Fe^{2+}$-entry. (D) Quench of Fura-2 fluorescence in Hela cells expressing TRPML1 stimulated with 20 μM MLSA1 and then 1 mM $FeCl_2$. Experiments were performed in nominally $Ca^{2+}$-free medium either in the presence of vehicle (0.1 % % DMSO) or 20 μM BTP2. (E) Summary data (124-144 cells). (F-G) Depletion of ER $Ca^{2+}$ stores does not evoke $Fe^{2+}$ entry. (F) Quench of Fura-2 fluorescence in Hela cells expressing TRPML1 stimulated with 1 mM $FeCl_2$ in the presence of vehicle (0.1 % DMSO) or 1 μM thapsigargin. (G) Summary data (84-130 cells).
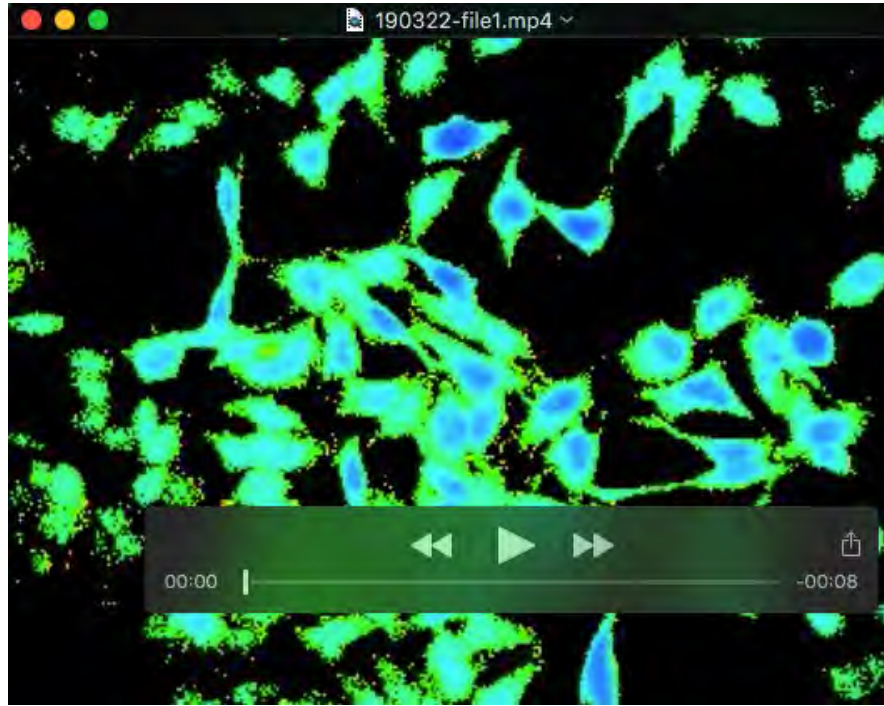
**Movie S1. Activation of TRPML evokes global Ca$^{2+}$ signals in Hela cells**. Effect of 20 µM ML-SA1 on cytosolic Ca$^{2+}$ levels of Fura-2 loaded Hela cells. Images were acquired every 3 s and played back at a rate of 40 frames per second. Warmer colours represent an increase in Fura-2 fluorescence ratio which is proportional to Ca$^{2+}$ concentration.
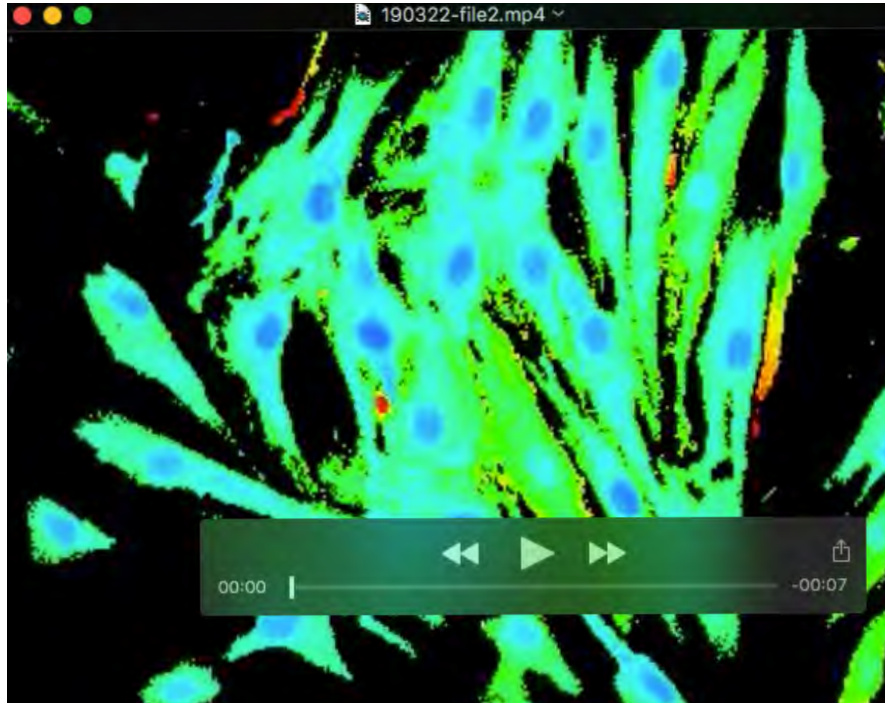
**Movie S2. Activation of TRPML evokes global Ca²⁺ signals in fibroblasts**. Effect of 20 µM ML-SA1 on cytosolic Ca²⁺ levels of Fura-2 loaded fibroblasts. Images were acquired every 3 s and played back at a rate of 40 frames per second. Warmer colours represent an increase in Fura-2 fluorescence ratio which is proportional to Ca²⁺ concentration.